PHOTON AND NEUTRAL PION DISTRIBUTIONS IN 60 AND 200 A GeV ^{16}O + NUCLEUS AND PROTON + NUCLEUS REACTIONS ☆

WA80 Collaboration

R. ALBRECHT [a], T.C. AWES [b], C. BAKTASH [b], P. BECKMANN [c], F. BERGER [c], R. BOCK [a], G. CLAESSON [a], L. DRAGON [c], R.L. FERGUSON [b], A. FRANZ [d], S. GARPMAN [e], R. GLASOW [c], H.A. GUSTAFSSON [e], H.H. GUTBROD [a], K.H. KAMPERT [c,1], B.W. KOLB [a], P. KRISTIANSSON [d], I.Y. LEE [b], H. LÖHNER [c], I. LUND [a,2], F.E. OBENSHAIN [b,f], A. OSKARSSON [e], I. OTTERLUND [e], T. PEITZMANN [c], S. PERSSON [e], F. PLASIL [b], A.M. POSKANZER [d], M. PURSCHKE [c], H.G. RITTER [d], R. SANTO [c], H.R. SCHMIDT [a], T. SIEMIARCZUK [a,3], S.P. SORENSEN [b,f], E. STENLUND [e] and G.R. YOUNG [b]

[a] *Gesellschaft für Schwerionenforschung (GSI), D-6100 Darmstadt, Fed. Rep. Germany*
[b] *Oak Ridge National Laboratory, Oak Ridge, TN 37831, USA*
[c] *University of Münster, D-4400 Münster, Fed. Rep. Germany*
[d] *Lawrence Berkeley Laboratory, Berkeley, CA 94720, USA*
[e] *University of Lund, S-22362 Lund, Sweden*
[f] *University of Tennessee, Knoxville, TN 37996, USA*

Received 2 December 1987

Transverse momentum (p_T) distributions of inclusive photons and neutral pions at midrapidity are measured with a lead glass calorimeter in 60 and 200 A GeV ^{16}O+ nucleus and proton + nucleus reactions. The variation of the average transverse momentum is investigated as function of centrality, determined by measurements of the remaining energy of the projectile and the charged particle multiplicity. For small values of the entropy, deduced from the multiplicity density, an increase in average p_T is observed levelling off for larger values of entropy. The target-mass and energy dependence of π^0 p_T distributions are presented.

Quantum chromodynamics lattice calculations [1] predict that at high nuclear density and high temperature a new phase of matter, the quark–gluon plasma (QGP) will be produced. The energy density necessary for deconfinement is estimated to be of the order of 2–3 GeV/fm^3 [2] which may be generated in heavy ion reactions at ultrarelativistic energies. First experimental results from ^{16}O + nucleus reactions [3,4] show that, in the most central events, energy densities above 2 GeV/fm^3 are reached. Since the signature of the QGP is not well established, measurements of both hadron–nucleus and nucleus–nucleus reactions have to be compared at different energies. Characteristic signals for the deconfinement phase transition [5,6] are expected from photon and lepton pair spectroscopy. Up to now, cosmic ray data have been the only source of information [7] and the observed rise of hadron transverse momenta with energy density has been interpreted as due to QGP effects [8]. In our experiment at the CERN SPS oxygen beams of 60 and 200 A GeV were used and, for comparison, p + nucleus data were taken with the same experimental setup at 60 and 200 GeV.

The details of the WA80 setup at the CERN SPS are given in ref. [9]. For the data presented in this letter the following components are of primary inter-

☆ One of us (R.S.) thanks the VW-Stiftung for the financial support during his stay at CERN in 1986.
1 Post Doctoral Fellowship from the German Research Community (DFG).
2 Post Doctoral Fellowship from Swedish Natural Research Science Council.
3 On leave of absence from the Institute of Nuclear Studies, PL-00681 Warsaw, Poland.

0370-2693/88/$ 03.50 © Elsevier Science Publishers B.V. (North-Holland Physics Publishing Division)

est: the electromagnetic lead glass calorimeter (SAPHIR), the uranium scintillator sampling calorimeter at zero degree (ZDC), and the streamer tube multiplicity arrays which cover the pseudorapidity region $1.2 \leqslant \eta \leqslant 4.2$.

The ZDC characterizes the centrality of each collision by measuring the remaining energy of projectile spectators for laboratory angles $\leqslant 0.3°$. A strong correlation between charged particle multiplicity and energy in ZDC is observed [10], so that both quantities may be used to distinguish between peripheral and central reactions.

SAPHIR measures the inclusive photon and π^0 distributions at midrapidity. Details of the construction and performance are given in table 1. Values for energy resolution and shower development at various angles of incidence were obtained from measurements at the DESY electron test beam (0.6–6 GeV) with a prototype detector. The complete SAPHIR setup has been tested and calibrated with electron and hadron beams (4–20 GeV) at the CERN SPS. The center of the front surface of the detector is located at 342 cm from the target and at an angle of 20° with respect to the beam direction. This gives an approximate pseudorapidity coverage of $1.5 \leqslant \eta \leqslant 2.1$ and a solid angle of 0.13 sr. Short term gain stability is continuously monitored with a nitrogen laser system. The long term stability is monitored with two independent NaI(Tl) crystals doped with Am. Light fibres conduct the laser light to the front surface of each lead glass element. The laser light intensity can be varied with filters to obtain the response of the photomultipliers over the full dynamic range and to evaluate the linearity corrections (< 5% max. deviation). The charged particle detection is achieved by two layers of plastic streamer tubes in front of the lead glass resulting in a 98% detection probability for charged particles. In order to enhance the statistics in the tail of the momentum distributions, SAPHIR is included in the trigger so that events with high energy photons are always recorded.

The streamer tube material contributes 4% to the photon conversion probability. The target vacuum chamber, a thin (500 μm) spherical aluminum chamber, contributes an additional 0.4%. Care was taken to keep all extraneous material out of the reaction zone, and background levels during target-out operation were found negligible. In addition, thin targets were used to minimize contributions from secondary interactions. The target thicknesses were 186 mg/cm^2 of C and 250 mg/cm^2 of Au, corresponding to an average photon conversion probability of 0.2% and 1.6% for C and Au, respectively. The π^0 acceptance includes the photon conversion probabilities and rises from 20% at low (0.6 GeV/c) values of the pion transverse momentum, p_T, to about 70% at 2 GeV/c and about 80% at 6 GeV/c. Error bars shown in π^0 momentum distributions include the contributions from acceptance correction uncertainties in addition to the statistical errors. The π^0 mass resolution $\sigma(M)/M$ is 5–8% (see fig. 1) and is limited mainly by variations in position resolution for different angles of incidence (non-projective geometry).

Inclusive spectra of photons, which dominantly originate from π^0 decay, have been extracted from the raw data under the following selection criteria:

(1) No hit of a charged particle is observed by the multiplicity detectors in the vicinity of a photon candidate.

(2) The transverse shower development is com-

Table 1
SAPHIR construction items and performance.

material	1278 lead glass modules SF5
module cross section	35×35 mm^2
module length	460 mm ≡ 18 radiation lengths (98% containment for 30 GeV photons)
total (rectangular) area	98×171.5 cm^2
spatial resolution	⩽ 5 mm (dependent on angle of incidence)
energy resolution	$(6/\sqrt{E/\mathrm{GeV}} + 0.4)\%$
gain stability	$(0.5 \pm 0.6)\%$
dynamic range	50 MeV – 25 GeV
minimum ionizing signal	540 MeV photon equivalent

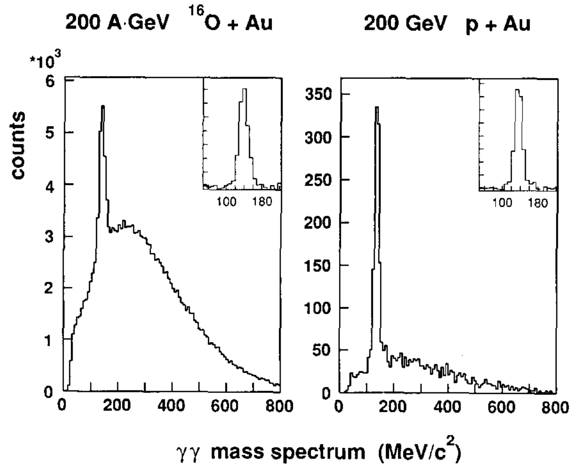

Fig. 1. Invariant mass spectra of γγ pairs for ^{16}O + Au and p + Au at 200 A GeV. Only photons with $E_\gamma > 500$ MeV and $p_{T\gamma\gamma} > 1$ GeV/c are considered. The insets show the π^0 peak after background subtraction.

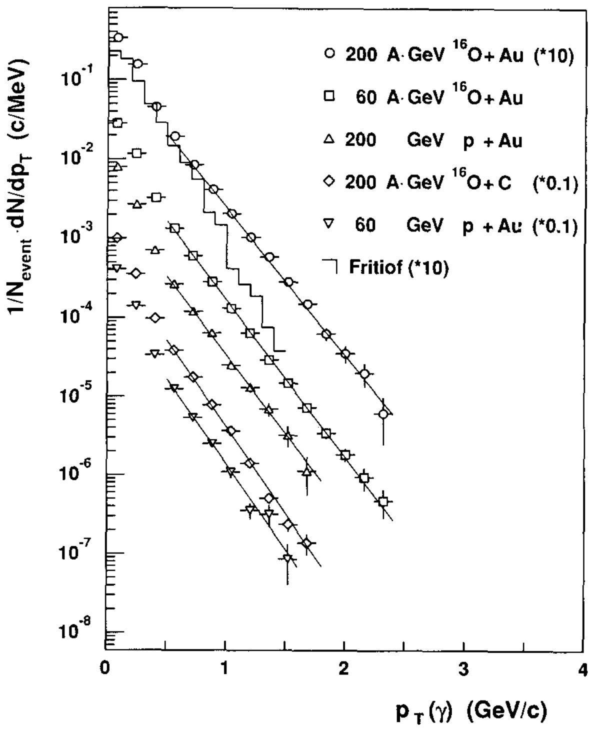

Fig. 2. Inclusive photon p_T distributions selected for central reactions with 10% of the minimum bias cross section. For comparison with exponential parametrizations (solid lines) the histogram shows the FRITIOF model results for ^{16}O+ Au at 200 A GeV.

patible with that of an electromagnetic (EM) model shower of the same energy and at the same point of incidence.

The EM model showers were derived from Monte Carlo simulations, and compare reasonably well with test beam data. Since there are too few modules involved in the shower development at photon energies below 0.5 GeV, this method of EM shower selection breaks down leading to systematic errors which are included in the error bars shown in the photon spectra. For p + Au and ^{16}O + Au reactions a maximum number of 19 and 45 hits per event, respectively, were observed at 200 A GeV. From the analysis of distance distributions of hits on the SAPHIR surface we estimate an average shower overlap probability of 2%.

Fig. 2 shows inclusive photon p_T spectra containing about 10% of the minimum bias cross section after a selection of events with high charged particle multiplicity. The data are well described by an exponential parametrization $dN/dp_T \sim \exp(-p_T/T_{eff})$ for $p_T > 0.4$ GeV/c. Table 2 contains the results of a fitting procedure for the data shown in fig. 2. The slope parameters T_{eff} increase slightly with increasing target- and projectile-mass and incident energy. The experimental data are compared with the Lund model for nucleus–nucleus interactions (FRITIOF) [11]. The predicted inverse slopes are in general about 20% lower than the slope parameters fitted to the data.

We have analyzed the p_T region above 0.4 GeV/c of the inclusive photon spectra as a function of target mass and event centrality, characterized by the energy measured in the ZDC, in the following ways:

(a) fitting an exponential to the dN/dp_T distributions,

(b) calculating the average p_T from the truncated p_T distributions [12] by integrating the experimental data:

Table 2
Slope parameters T_{eff} in MeV/c from an exponential fitting procedure [$dN/dp_T \sim \exp(-p_T/T_{eff})$] for $p_T > 0.4$ GeV/c applied to the data shown in fig. 2. Errors are statistical errors only as obtained from the fit procedure.

Energy per nucleon (GeV)	p + Au	^{16}O + C	^{16}O + Au
60	198±3	181±2	215±2
200	215±4	193±3	234±2

$$\langle p_T \rangle_{\gamma,C} = \left(\int_C^\infty p_T \frac{dN}{dp_T} dp_T \Big/ \int_C^\infty \frac{dN}{dp_T} dp_T \right) - C, \tag{1}$$

using $C=400$ MeV/c. Both methods give equivalent results. An example using method (b) is shown in fig. 3. Here, an increase in $<p_T>_{\gamma,400}$ of 15% is observed for 200A GeV ^{16}O + Au as function of the centrality as measured by the energy in the zero degree calorimeter. For the lighter systems the increase is less pronounced and lower values are observed for the lower incident energy. The FRITIOF model predicts almost no variation with centrality or target mass, however, it tends to be closer to the experiment for peripheral oxygen induced reactions and for proton induced reactions. Since the low p_T part of the spectrum tends to influence the results, the absolute numbers of $\langle p_T \rangle_{\gamma,C}$ are, of course, dependent on the choice of the cutoff value C. We find a shift in the absolute $\langle p_T \rangle_{\gamma,C}$ scale of -4% ($+$ 4%) when C is changed by -80 MeV ($+120$ MeV) leaving the observed centrality dependence unchanged. Thus, the deviation from FRITIOF is obvious, although it has to be noted, that in this model hard scattering [13] is not yet included for nucleus–nucleus reactions, which may account for part of the observed effect [14].

For proton projectiles the centrality of the reaction is not well defined by the ZDC energy. In order to compare the oxygen and proton induced reactions properly and to relate the data in fig. 3 to thermodynamical models [15], we have used the entropy density [15,16] which is, except for a constant factor, given by $S=(dN/d\eta)A_{\rm inc}^{-2/3}$. Here $dN/d\eta$ is the central multiplicity density which is approximated by the charged particle multiplicity in $1.2<\eta<4.2$ for different intervals in ZDC energy multiplied by 1.5 in order to correct for undetected neutral particles. $A_{\rm inc}$ is the mass number of the smaller colliding nucleus in central collisions. For peripheral heavy ion collisions, however, this assumption is no longer justified. Therefore $A_{\rm inc}$ is defined to be the number of incident projectile participants, which is derived from the ZDC energy via the FRITIOF model in close resemblance to ref. [4]. In this way the most peripheral oxygen data are expected to correspond to the proton data.

With this assumption the $\langle p_T \rangle_{\gamma,400}$ of photons as a function of the entropy density is plotted in fig. 4. We observe an increase of $\langle p_T \rangle_{\gamma,400}$ with entropy density S. Different from the proton induced reactions, the ^{16}O + Au data extend to large values of S ($S>10$)

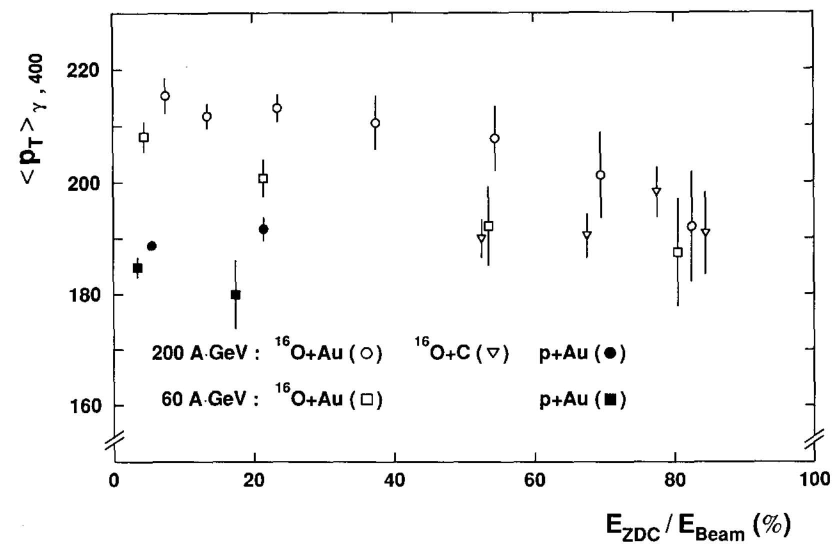

Fig. 3. Experimental $\langle p_T \rangle_{\gamma,400}$ for inclusive photons from the truncated p_T distribution (see text) as function of centrality of the reaction defined by the energy deposited in the ZDC in percent of the beam energy.

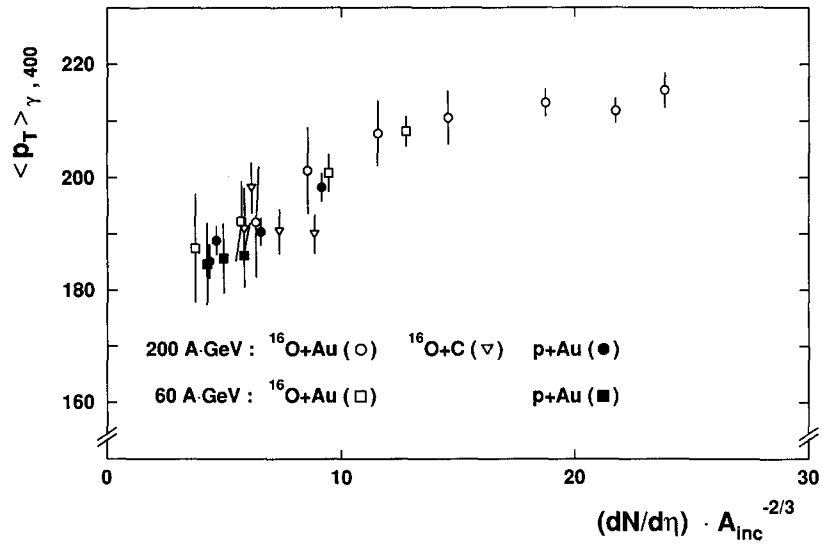

Fig. 4. Experimental $\langle p_T \rangle_{\gamma,400}$ for inclusive photons from the truncated p_T distribution (see text) as function of the entropy density estimated from the central charged particle multiplicity and the number of participating projectile nucleons which is calculated from the energy in the ZDC.

with increasing beam energy. The data points at highest S contain between 10 and 30% of the minimum bias cross section. A remarkable feature of fig. 4 is the small increase of $\langle p_T \rangle_{\gamma,400}$ at intermediate and large values of the entropy density S for ^{16}O + Au reactions at 200 A GeV. At low entropy density ($S<$ 10) the rise of $\langle p_T \rangle_{\gamma,400}$ may even be enhanced by up to 6% due to possible systematic errors in the photon identification. A structure like this is expected from thermodynamical and hydrodynamical studies [15,17,18] of the QGP phase transition and is reminiscent of earlier observations of cosmic ray data [7]. The relative variation of $\langle p_T \rangle_{\gamma,400}$ for p + Au at 200 GeV is consistent with data obtained from p+p and $\alpha+\alpha$ reactions at the ISR [19]. The increase to larger values of $\langle p_T \rangle$ in p+$\bar{p}$ collider data [20], where equivalently large entropy values are reached, is more closely related to the ^{16}O + Au data than to the p + Au data.

Invariant cross sections for π^0 have been obtained by analysing the invariant mass spectra of $\gamma\gamma$ pairs in small intervals of p_T. The combinatorial background below the invariant mass peak was fitted by a third order polynomial and after subtraction leads to a gaussian π^0 mass peak (fig. 1). The obtained π^0 cross sections from p + Au reactions compare within the error limits to Fermilab data [21] for π^+ and π^- from p+ W at the same incident energy and in approximately the same region of rapidity.

In fig. 5 the p_T dependence of invariant π^0 cross sections for minimum bias trigger conditions from proton and oxygen induced reactions is compared for different targets and energies. The slopes of these distributions for $p_T>$ 0.8 GeV/c can be described by an exponential parametrization $[(1/p_T)\ dN/dp_T \sim \exp(-p_T/T_0)]$, and slope parameters T_0 have been deduced from the same restricted transverse momentum range 0.8 GeV/$c \leqslant p_T \leqslant 2$ GeV/c for all reaction systems (table 3). The slope parameters turn out to be similar for proton and oxygen induced reactions

Table 3
Slope parameters T_0 in MeV/c for an exponential parametrization of invariant cross sections $[(1/p_T)dN/dp_T \sim \exp(-p_T/T_0)]$ for π^0 production in $1.5 \leqslant \eta \leqslant 2.1$ and for 0.8 GeV/$c \leqslant p_T \leqslant 2$ GeV/c as a function of target and projectile mass and beam energy. Errors originate from statistics and acceptance correction.

Energy per nucleon (GeV)	p + Au	^{16}O + C	^{16}O + Au
60	179±13	186±8	200±7
200	196± 8	190±7	210±5

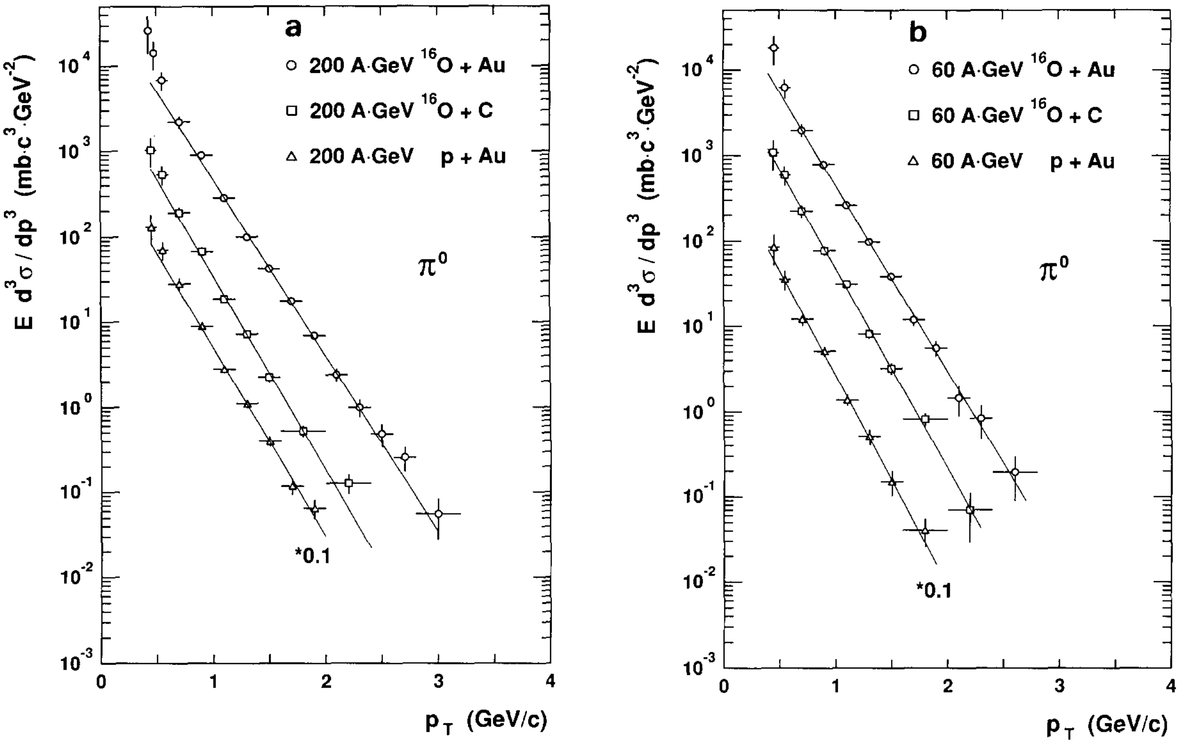

Fig. 5. Invariant cross sections for π^0 as a function of p_T from proton and oxygen induced reactions at 200 (a) and 60 *A* GeV (b) measured in $1.5 \leqslant \eta \leqslant 2.1$ for different target masses.

in these minimum bias data and are only weakly dependent on target mass, but are larger by at least 20% for ^{16}O + Au at 200 *A* GeV than for p + p reactions [22] and for FRITIOF model predictions. This behaviour is consistent with the observations cited above which show that the linear extrapolation from p + p reactions to heavy ion reactions, as contained in this model, is doubtful. In order to exclude effects from a change in the effective center-of-mass (CM) system when proton and oxygen induced reactions are compared, we investigated the η-dependence for ^{16}O + Au at 200 *A* GeV within the acceptance of SAPHIR ranging from 1.5 to 2.1 in η. No significant change in slope in this interval is observed which is larger than the expected change in the effective CM system.

The spectra in fig. 5 show a change in slope below $p_T \simeq 0.8$ GeV/*c*, which is most pronounced for the heavy system. A slope parameter $T_0 \leqslant 150$ MeV/*c* would be appropriate to describe the data for $p_T < 0.8$ GeV/*c*. This effect is not seen in 250 GeV/*c* p + p reactions [22], but is consistent with $\alpha+\alpha$ reactions at the ISR [12,19,23] and weakly indicated in the p+ Au data at 200 GeV. This feature is also predicted in thermodynamical models [18,24] and in studies of the hydrodynamical expansion [17,25] of the QGP.

In summary, it has been shown that even in the high multiplicity environment of ^{16}O + Au reactions the identification of π^0 in the invariant mass spectrum of $\gamma\gamma$ pairs is achieved with good accuracy in a lead glass detector. Inclusive photon spectra and p_T distributions for identified π^0 have been presented for 60 and 200 *A* GeV ^{16}O + nucleus and p + nucleus reactions.

The photon spectra show a target mass and centrality dependence in the region $p_T > 0.4$ GeV/*c* which is not predicted by the current FRITIOF model. Reactions with different initial geometry can be compared with each other when $\langle p_T \rangle$ is plotted as a function of the entropy density calculated from the multiplicty and the number of projectile participants. The levelling off of a purely linear increase of

$\langle p_T \rangle_{\gamma,400}$ with entropy density for ^{16}O + Au at 200 A GeV reveals features expected in the presence of a phase transition.

The π^0 p_T distributions show at least two components, a low p_T one with an inverse slope of about 150 MeV/c and a high p_T component with a flatter slope dependent slightly on target mass. These features are not compatible with a FRITIOF type linear extrapolation from p + p data to heavy ion reactions. A description in terms of a thermodynamical evolution and hydrodynamical expansion of a hot hadronic system seems to be justified and could be used for quantitative comparisons. Nevertheless, hard scattering of partons needs to be included in nucleus–nucleus scattering models, in order to study if the above observations can be explained within refined non-thermal models.

We gratefully acknowledge the support by Professor Foa (Università di Pisa), for providing us with additional lead glass modules, and by Professor Duhm, Professor Scobel, Dr. Strauss and Dr. Krause from University Hamburg during the DESY test experiments. Partial support by the West German BMFT and DFG, the United States DOE, the Swedish NFR, the Humboldt Foundation and the CERN EP-division is gratefully acknowledged.

References

[1] L. McLerran and B. Svetitsky, Phys. Lett. B 98 (1981) 195; T. Celik, J. Engels and H. Satz, Nucl. Phys. B 256 (1985) 670.
[2] M. Jacob and H. Satz, eds., Quark matter formation and heavy ion collisions, proc. Bielefeld Workshop (May 1982) (World Scientific, Singapore, 1982).
[3] A. Bamberger et al., Phys. Lett. B 184 (1987) 271.
[4] WA80 Collab., R. Albrecht et al., Phys. Lett. B 199 (1987) 297.
[5] R.C. Hwa and K. Kajantie, Phys. Rev. D 32(1985) 1109.
[6] S. Raha and B. Sinha, Phys. Rev. Lett. 58 (1987) 101.
[7] T.H. Burnett et al., Phys. Rev. Lett. 57 (1986) 3249.
[8] E.V. Shuryak and O.V. Zhirov, Phys. Lett. B 171 (1986) 99.
[9] H.H. Gutbrod et al., GSI preprint GSI-85-32 (August 1985), CERN SPSC/85-39/M406
[10] WA80 Collab., I. Lund et al., contrib. 6 Intern. Conf. on Ultra-relativistic nucleus–nucleus collisions (Schloss Nordkirchen, 1987), Z. Phys. C, to be published.
[11] B. Nilsson-Almqvist and E. Stenlund, Comput. Phys. Commun. 43 (1987) 387.
[12] W. Bell et al., Z. Phys. C 27 (1985) 191.
[13] M. Lev and B. Petersson, Z. Phys. C 21 (1983) 155.
[14] B. Nilsson-Almqvist, contrib. High energy physics 87 Conf. (Uppsala, 1987).
[15] L. van Hove, Nucl. Phys. A 447 (1985) 443c.
[16] J.D. Bjorken, Phys. Rev. D 27 (1983) 140.
[17] M. Kataja et al., Phys. Rev. D 34 (1986) 2755.
[18] E.V. Shuryak, Phys. Rep. 61 (1980) 71.
[19] A. Breakstone et al., Phys. Lett. B 183 (1987) 227.
[20] UA1 Collab., G. Arnison et al., Phys. Lett. B 118 (1982) 167.
[21] D. Antreasyan et al., Phys. Rev. D 19 (1979) 764.
[22] NA22 Collab., P. van Hal, Thesis, CERN (1987).
[23] A.L.S. Angelis et al., Phys. Lett. B 185 (1987) 213.
[24] M. Danos and J. Rafelski, Phys. Rev. D 27 (1983) 671.
[25] J.P. Blaizot and J.Y. Ollitrault, Phys. Lett. B 191 (1987) 21.